

Activation of GPR55 Ameliorates Maternal Separation-Induced Learning and Memory Deficits by Augmenting 5-HT Synthesis in the Dorsal Raphe Nucleus of Juvenile Mice

Ting Sun, Ya-Ya Du, Yong-Qiang Zhang, Qin-Qin Tian, Xi Li, Jiao-Yan Yu, Yan-Yan Guo, Qing-Qing Liu, Le Yang, Yu-Mei Wu, Qi Yang,* and Ming-Gao Zhao*



Cite This: *ACS Omega* 2024, 9, 21838–21850



Read Online

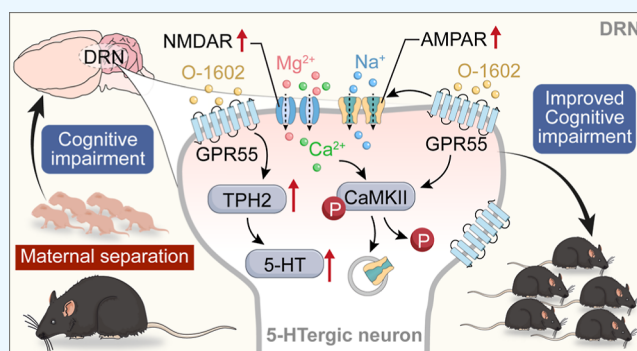
ACCESS |

Metrics & More

Article Recommendations

Supporting Information

ABSTRACT: Maternal separation (MS) represents a profound early life stressor with enduring impacts on neuronal development and adult cognitive function in both humans and rodents. MS is associated with persistent dysregulations in neurotransmitter systems, including the serotonin (5-HT) pathway, which is pivotal for mood stabilization and stress-coping mechanisms. Although the novel cannabinoid receptor, GPR55, is recognized for its influence on learning and memory, its implications on the function and synaptic dynamics of 5-HT neurons within the dorsal raphe nucleus (DRN) remain to be elucidated. In this study, we sought to discern the repercussions of GPR55 activation on 5-HT synthesis within the DRN of adult C57BL/6J mice that experienced MS. Concurrently, we analyzed potential alterations in excitatory synaptic transmission, long-term synaptic plasticity, and relevant learning and memory outcomes. Our behavioral assessments indicated a marked amelioration in MS-induced learning and memory deficits following GPR55 activation. In conjunction with this, we noted a substantial decrease in 5-HT levels in the MS model, while GPR55 activation stimulated tryptophan hydroxylase 2 synthesis and fostered the release of 5-HT. Electrophysiological patch-clamp analyses highlighted the ability of GPR55 activation to alleviate MS-induced cognitive deficits by modulating the frequency and magnitude of miniature excitatory postsynaptic currents within the DRN. Notably, this cognitive enhancement was underpinned by the phosphorylation of both NMDA and α -amino-3-hydroxy-5-methyl-4-isoxazolepropionic acid (AMPA) receptors. In summary, our findings underscore the capacity of GPR55 to elevate 5-HT synthesis and modify synaptic transmissions within the DRN of juvenile mice, positing GPR55 as a promising therapeutic avenue for ameliorating MS-induced cognitive impairment.



1. INTRODUCTION

Early life stress (ELS) can lead to permanent changes in neurodevelopment,^{1–3} which may increase the risk of psychopathology in adulthood.^{4–6} Both human and animal studies have suggested a strong link between early life trauma and psychopathology.^{7–9} Maternal separation (MS) is a commonly used method to simulate postnatal stress in experimental animals.¹⁰ Even during the stress hyporesponsive period, characterized by minimal response to most adult stressors, prolonged MS can exert considerable adverse effects. MS has been found to cause behavioral abnormalities resembling psychotic-like symptoms, such as disruption in the prepulse inhibition response,¹¹ neuroendocrine alterations associated with stress reactivity,^{12,13} and cognitive impairment in juvenile animals.^{2,3,14}

Various neurotransmitter systems, such as glutamatergic, dopaminergic, and serotonergic activities, can undergo alterations following MS.^{13,15–17} Serotonin (5-HT) plays a crucial role in both maturation during sensitive periods and learning-

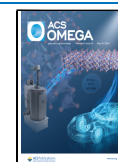
related neuroplasticity,¹⁸ suggesting that inherent differences in the central serotonergic signaling may impact the long-term consequences of ELS. The dorsal raphe nucleus (DRN) serves as the primary site for 5-HT synthesis in the brain, with elevated expression of tryptophan hydroxylase 2 (TPH2), a key enzyme responsible for 5-HT synthesis, in this region.¹⁹ Previous studies have identified a correlation between memory performance and extracellular 5-HT level in this system, and depleting tryptophan may impact memory formation.^{20,21} The biosynthesis of 5-HT is regulated by the rate-limiting enzyme TPH2, and increased mRNA expression of TPH2 has been shown to enhance TPH2

Received: November 9, 2023

Revised: April 16, 2024

Accepted: April 24, 2024

Published: May 7, 2024



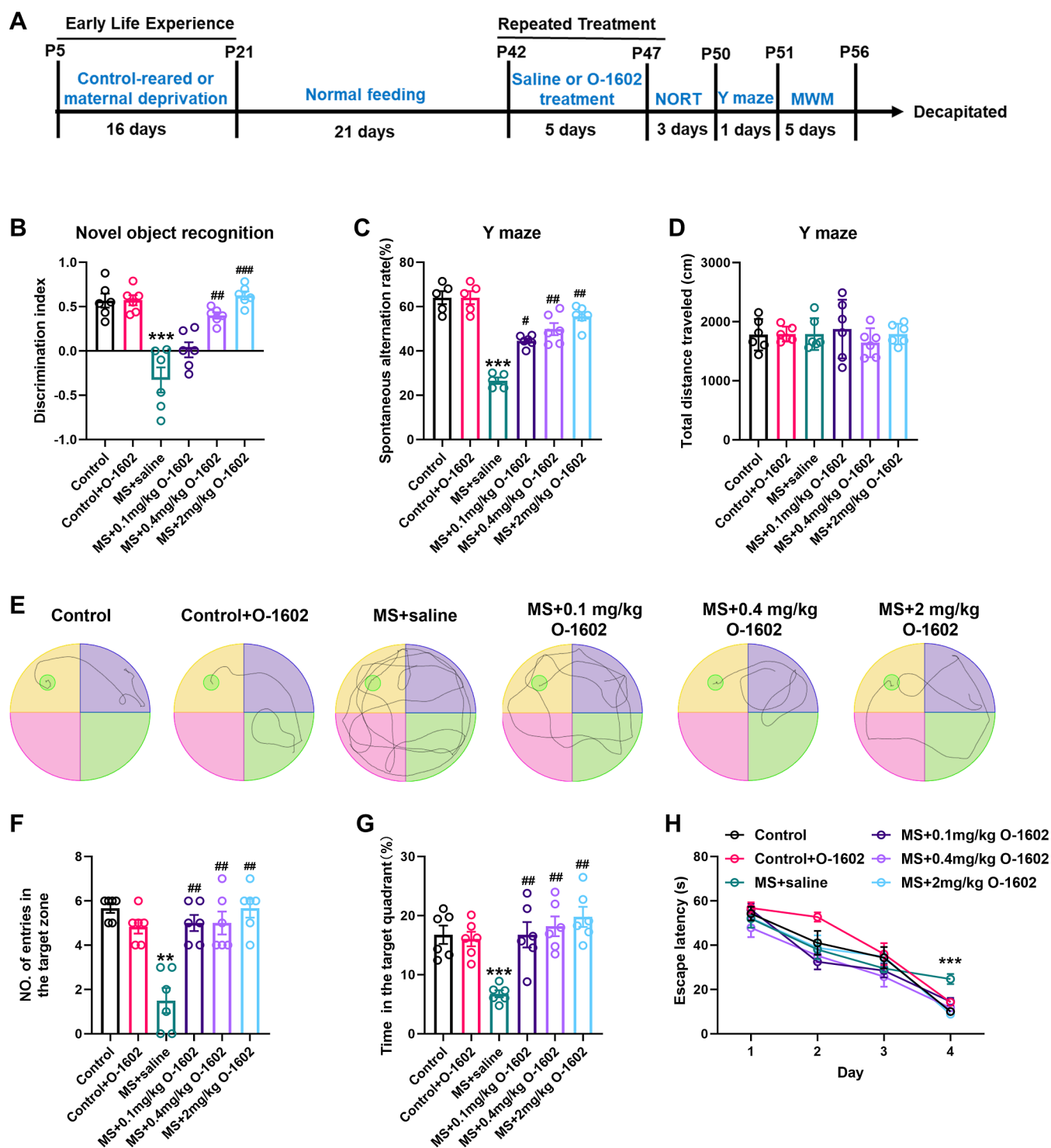


Figure 1. GPR55 agonist O-1602 protects mice against MS-induced learning and memory impairment. (A) Schematic representation of the experimental timeline detailing the establishment of the MS model, O-1602 treatment, and behavioral tests. We randomly divided the mice into the following groups: control, control + O-1602, MS + saline, MS + 0.1 mg/kg O-1602, MS + 0.4 mg/kg O-1602, and MS + 2 mg/kg O-1602 groups. (B) NORT shows the discrimination index of the different groups at 24 h ($n = 6$ mice per group). (C,D) Total distance traveled (cm) and percentage of spontaneous arm alternations in the Y-maze test ($n = 6$ mice per group). (E) Representative track images of mice in the probe trial of the MWM test. (F,G) Number of entries to the target zone and time spent in the target quadrant in the probe trial of the MWM test ($n = 6$ mice per group). (H) Escape latency to the platform during the training trial in the MWM test ($n = 6$ mice per group). All data are shown as mean \pm standard error of the mean (S.E.M); ** $p < 0.01$, *** $p < 0.001$ vs control group; # $p < 0.05$, ## $p < 0.01$, ### $p < 0.001$ vs MS group.

activity and subsequent 5-HT synthesis.^{22,23} Through selective inactivation of TPH2 in distinct subsets of 5-HTergic neurons within the dorsal and median raphe, researchers can gain better insights into the function of various subpopulations of 5-HT

neurons, which target diverse brain regions implicated in the regulation of cognition and emotionality.²⁴

The endocannabinoid system is a neuromodulatory system that regulates emotional, cognitive, and motor processes. The

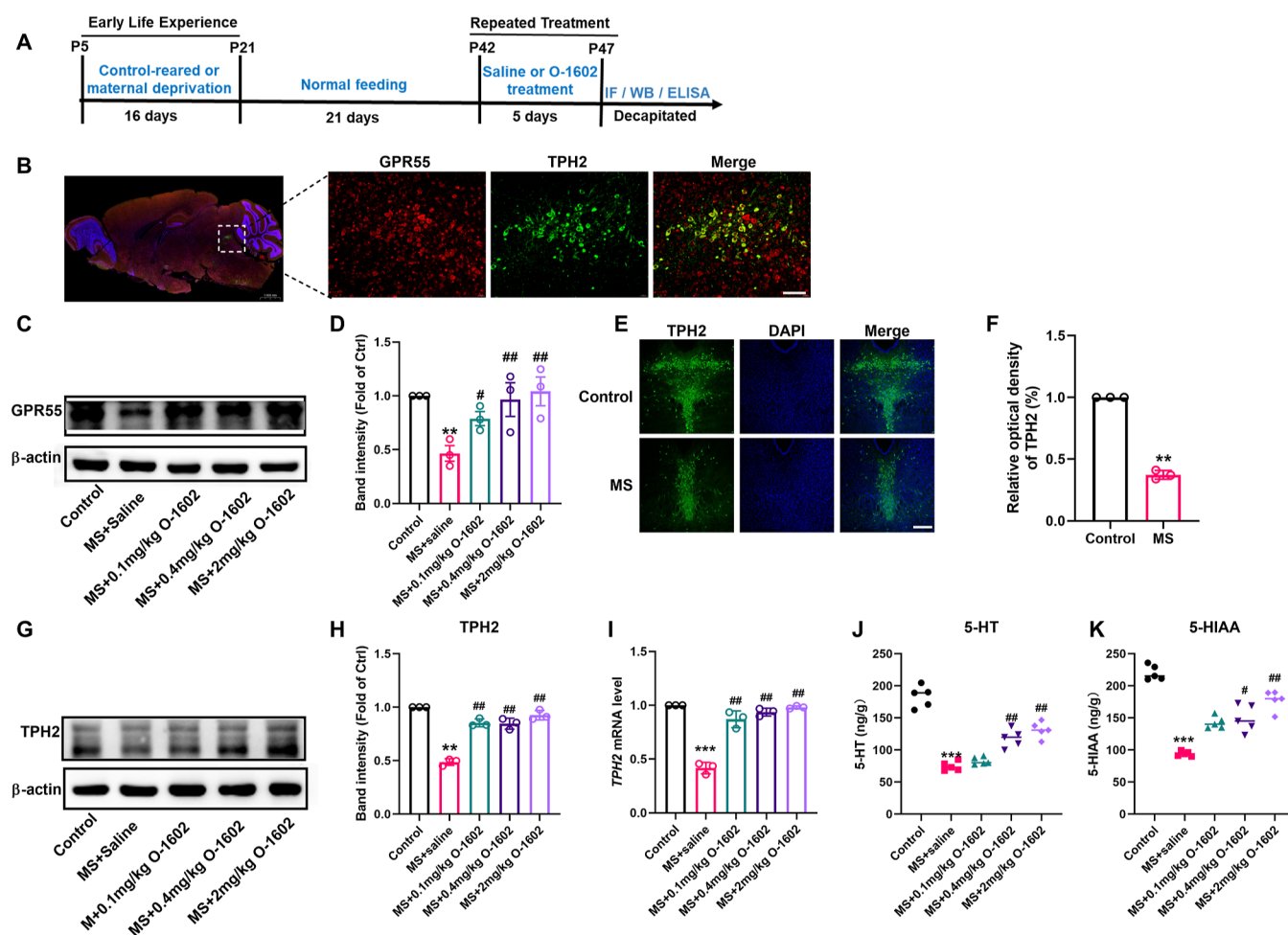


Figure 2. GPR55 activation promotes 5-HT synthesis and release of the 5-HT transmitter. (A) Schematic representation of the experimental timeline. (B) Representative images showing double immunostaining of GPR55 (red) and TPH2 (green) in the DRN of control mice ($n = 3$ mice per group). Scale bar = 100 μm . (C,D) Representative western blot images and densitometric analysis of GPR55 protein expression in the DRN ($n = 3$ mice per group). (E) Representative immunofluorescent images of TPH2 staining of the control and MS groups. Scale bar = 100 μm . (F) Immunofluorescence density in 5-HT neurons by image J ($n = 3$ mice per group). (G,H) Representative western blot images and densitometric analysis of TPH2 protein expression in the DRN ($n = 3$ mice per group). (I) Effects of MS on the mRNA level of *TPH2* in the DRN ($n = 3$ mice per group). (J,K) Enzyme-linked immunosorbent assay (ELISA) results show the levels of amino acid neurotransmitters 5-HT and 5-HIAA in the DRN of the control, MS + saline, MS + 0.1 mg/kg O-1602, MS + 0.4 mg/kg O-1602, and MS + 2 mg/kg O-1602 groups ($n = 5$ mice per group). All data are shown as mean \pm S.E.M; $**p < 0.01$, $***p < 0.001$ vs control group; $\#p < 0.05$, $\#\#p < 0.01$ vs MS group.

antidepressant effect mediated by cannabinoid subtype 1 receptor activation is primarily associated with the levels of 5-HT and noradrenaline,²⁵ as well as neurogenesis and synaptic plasticity enhancement.²⁶ Cannabinoid subtype 1 receptor activation has been found to inhibit synaptic transmission in the basolateral amygdala-nucleus accumbens neural circuit and activate extracellular regulated protein kinase 1/2.²⁷ GPR55, a novel cannabinoid receptor, exhibits a high affinity for cannabinoid ligands. It is expressed in various tissues in mice, including the nervous system (i.e., hippocampus, striatum, amygdala, and cortex) and peripheral tissues, such as endothelial cells and the gastrointestinal tract.^{29,30} GPR55 agonists exert a neuroprotective effect in Parkinson's disease,^{31,32} anxiety,³³ pain perception,³⁴ and axon innervation and guidance.^{35,36} GPR55 activation protects pancreatic β -cells against endoplasmic reticulum stress-induced apoptosis.³⁷ In addition, GPR55 activation may reverse $A\beta$ 1–42-induced cognitive impairment and neurotoxicity in mice by inhibiting the Rho subfamily protein A/Rho-related curly junction protein kinase 2 path-

way.^{38,39} However, no study has investigated whether activation of GPR55 can mitigate MS-induced cognitive dysfunction.

In this study, we sought to elucidate the effects of MS-induced learning and memory impairments on GPR55 expression within the DRN in juvenile mice. In addition, we investigated the potential protective role of the GPR55 agonist O-1602 as a treatment against cognitive deficits induced by MS. We also evaluated the recovery effect of O-1602 treatment on irregular 5-HT transmission in the DRN following MS. Our data revealed that activation of GPR55 increased the levels of 5-HT synthetase, facilitating an enhanced release of the 5-HT neurotransmitter. This culminated in a significant mitigation of MS-induced cognitive impairments. Our results offer a compelling rationale for exploring GPR55 as a therapeutic target for addressing learning and memory deficits associated with MS.

2. RESULTS

2.1. GPR55 Activation Mitigates Learning and Memory Impairment Induced by MS. To investigate the role of GPR55 in the learning and memory impairment induced by

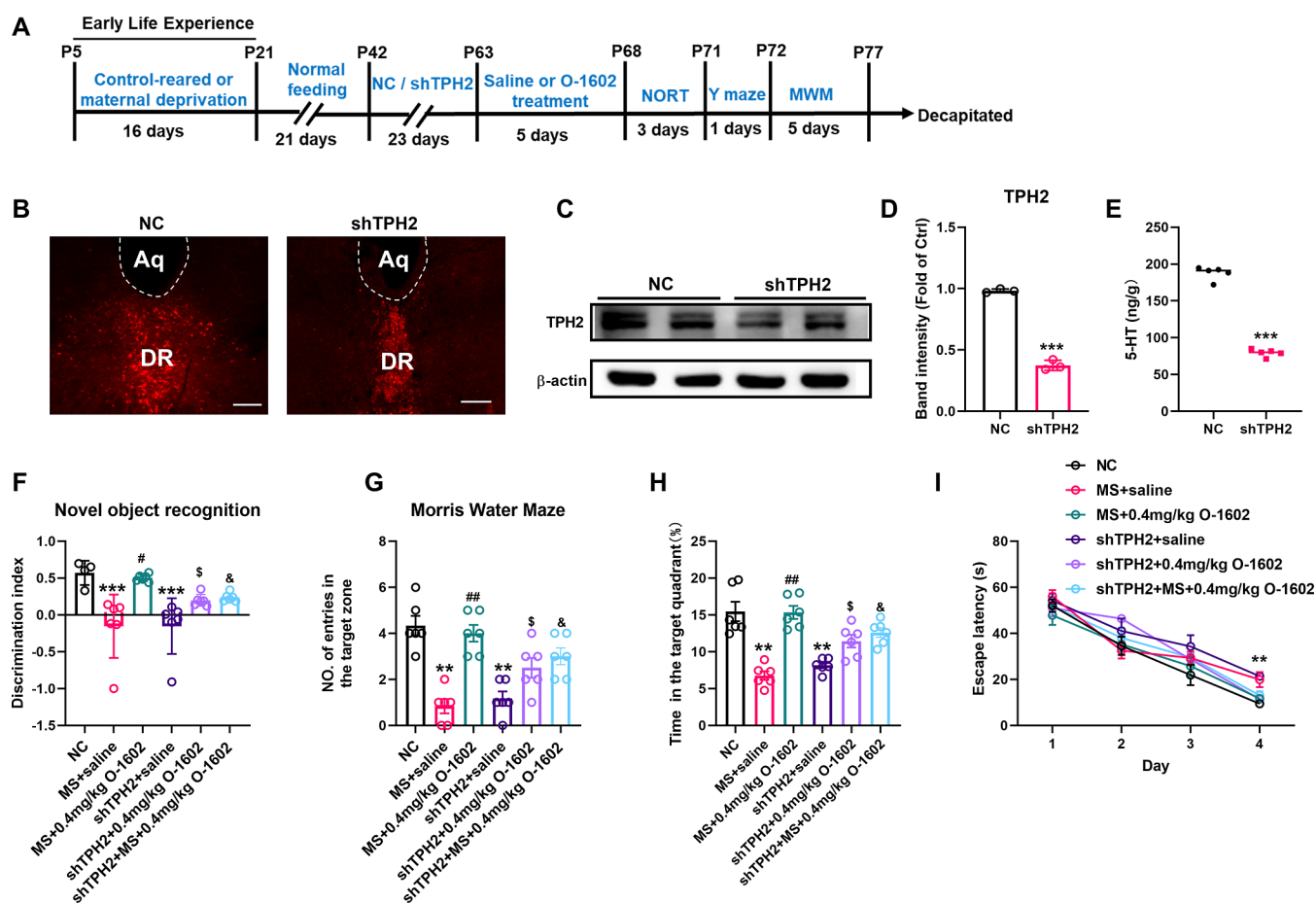


Figure 3. TPH2^{DRN} knockdown reduced the effect of GPR55 agonist on learning and memory in MS mice. (A) Schematic representation of the experimental timeline. (B) Representative confocal images of the mouse DRN after AAV injections. Scale bars = 100 μ m. (C,D) Representative western blot images and densitometric analysis of TPH2 protein expression in the DRN after AAV injections ($n = 3$ mice per group). (E) ELISA results show the concentrations of amino acid neurotransmitter 5-HT in the DRN of NC and shTPH2 mice ($n = 5$ mice per group). (F) NORT shows the discrimination index of the NC, MS, MS + 0.4 mg/kg O-1602, shTPH2, shTPH2 + 0.4 mg/kg O-1602, and shTPH2 + MS + 0.4 mg/kg O-1602 groups at 24 h ($n = 6$ mice per group). (G,H) Number of entries to the target zone and time spent in the target quadrant in the probe trial of the MWM test ($n = 6$ mice per group). (I) Escape latency to the platform during the training trial in the MWM test ($n = 6$ mice per group). All data are shown as mean \pm S.E.M.; ** $p < 0.01$, *** $p < 0.001$ vs control or NC group. # $p < 0.05$, ## $p < 0.01$ vs MS; \$ $p < 0.05$ vs shTPH2; & $p < 0.05$ vs MS + O-1602.

ELS, we first established a MS mouse model. After 16 days of MS, the mice were kept for an additional 21 days until they reached young adulthood [postnatal day (PND) 42–47]. Following this, the mice (PND 42 ± 2) were intraperitoneally injected with varying concentrations of O-1602, a selective GPR55 agonist, for five consecutive days, after which all behavioral tests were conducted. At first, the novel object recognition test (NORT) was performed after 24 h of training, indicating that mice from the MS group manifested a distinct decline in object location memory relative to the controls. This was evident in their recognition index (RI), where MS mice showed a significant decrease, indicating their reduced propensity to explore the novel object ($F_{(5, 30)} = 22.17$, $P < 0.0001$, Figure 1A,B). While a dosage of 0.1 mg/kg of O-1602 did not significantly alter the MS-induced cognitive deficits, dosages of 0.4 and 2.0 mg/kg notably mitigated these impairments ($P < 0.0001$). The Y-maze test, geared toward assessing spatial and working memory, demonstrated a marked decrease in the spontaneous alternation behavior of MS mice (PND 42 ± 2) ($P < 0.0001$). Notably, the overall distance traversed did not present any significant disparity. Moreover, the test reflected a considerable impairment in the working memory of these mice ($F_{(5, 27)} = 36.39$, $P < 0.0001$, Figure 1C,D).

Nonetheless, the concentrations of 0.1, 0.4, and 2.0 mg/kg O-1602 administration resulted in a marked enhancement in the cognitive performance of MS mice. Using the Morris water maze (MWM) to evaluate spatial learning, it was observed that MS mice required a longer duration (escape latency) to identify the platform in comparison to controls ($F_{(5, 28)} = 15.63$, $P < 0.0001$, Figure 1E,F). Furthermore, MS mice exhibited compromised memory functions during the probe trial, as evidenced by their reduced time spent in the target quadrant and fewer platform crossings than control mice ($F_{(5, 30)} = 8.702$, $F_{(5, 30)} = 14.24$, $P < 0.0001$, Figure 1G,H). Remarkably, the doses of 0.1, 0.4, and 2.0 mg/kg O-1602 treatment counteracted these behavioral discrepancies seen in MS mice. Meanwhile, after treatment with 0.4 mg/kg O-1602, the behavioral analysis of control mice had no significant changes. Our data underscores that GPR55 activation through O-1602 plays a pivotal role in counteracting the learning and memory deficits elicited by MS.

2.2. GPR55 Activation Promotes the Synthesis and Release of the 5-HT Transmitter. GPR55 is a cannabinoid- and lysophosphatidylinositol-sensitive receptor that is expressed throughout the central nervous system and can boost the release of neurotransmitters.^{30,40} 5-HT is an important neurotransmitter involved in learning and memory. Recent studies have shown

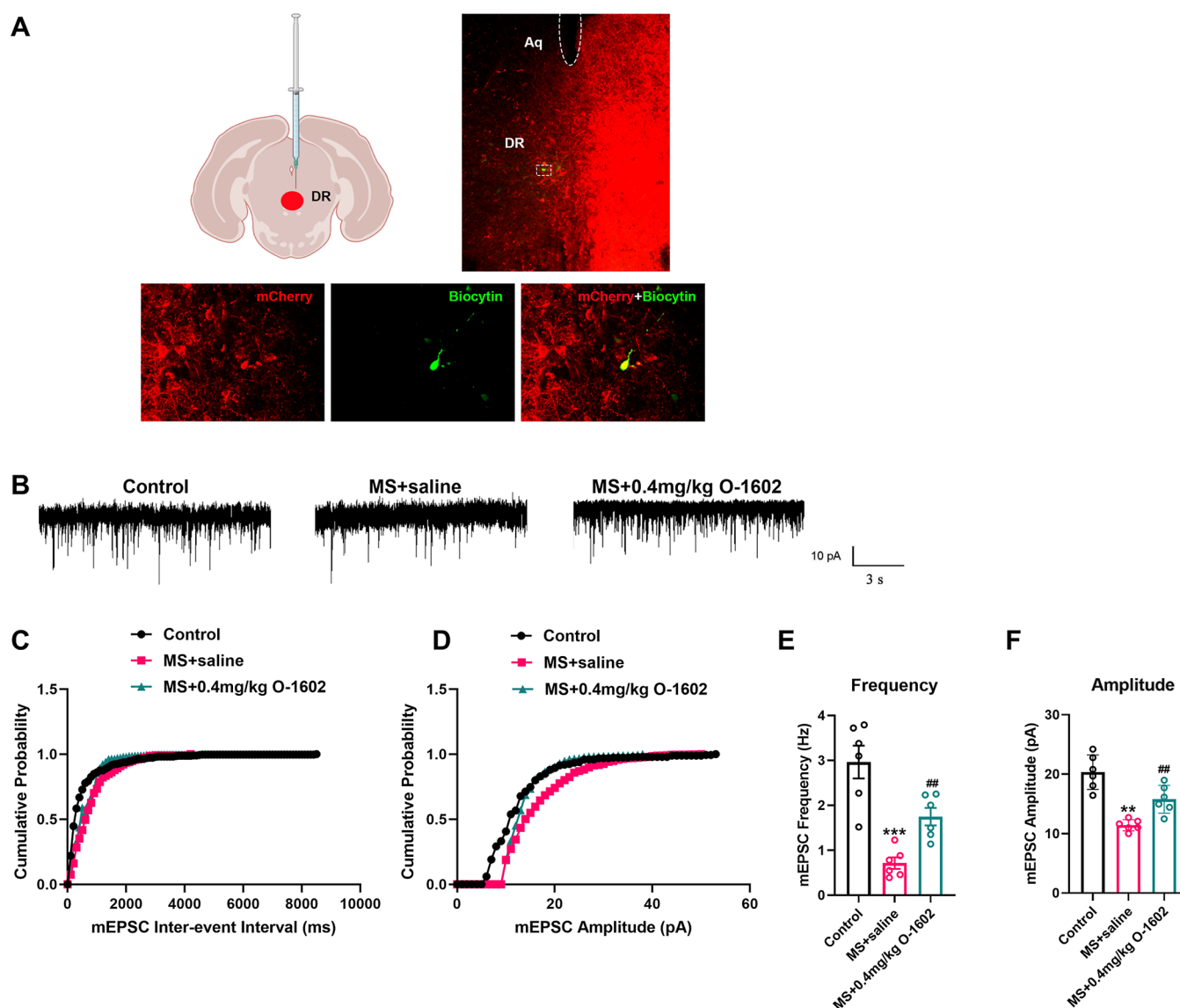


Figure 4. O-1602 reversed MS-induced reduction of excitatory synapse transmission in the DRN. (A) One representative whole-cell-patched neuron in the DRN was injected with biocytin (labeled with Alexa 488, green). Representative autofluorescence of the hM3Dq + TPH2 groups were labeled with red. Scale bars = 100 μ m (above) and 25 μ m (below). (B) Representative electrophysiological traces of spontaneous synaptic transmission in the DRN. (C,D) Cumulative frequency (C) and amplitude (D) histograms of the mEPSCs recorded from cells in each group. (E,F) Summary of mEPSC frequency (E) and amplitude (F) in neurons from mice ($n = 7$ neurons/3 mice in the control group; $n = 9$ neurons/3 mice in the MS + saline group; $n = 9$ neurons/3 mice in the MS + O-1602 group). All data are shown as mean \pm S.E.M; * $p < 0.05$, ** $p < 0.01$, *** $p < 0.001$ vs control group; # $p < 0.05$, ## $p < 0.01$, ### $p < 0.001$ vs MS group.

that 5-HTergic neurons mainly distributed in the DRN region are essential in early postnatal development, influencing the maturation and modulation of higher-order emotional, sensory, and cognitive circuitry.^{41–44} Thus, the connection between GPR55 and the 5-HT transmitter release was given priority.

First, we found that GPR55 was almost entirely colabeled with TPH2 (a marker of 5-HTergic neurons and an initial and rate-limiting enzyme for 5-HT synthesis) in the mouse DRN region via immunofluorescence staining (Figure 2A,B). Then, western blotting results indicated that the expression level of GPR55 in the DRN of MS mice (on the 16th day) was significantly reduced, and intraperitoneal injection of different concentrations of GPR55 agonist O-1602 could significantly increase the expression level of GPR55 ($F_{(4,10)} = 5.402$, $P < 0.0001$, Figure 2C,D). Next, we further investigated whether GPR55 activation can regulate 5-HT synthesis. In contrast to the control

group, a significant reduction in 5-HTergic neurons was observed in MS mice (Figure 2E,F, $P < 0.0001$). The levels of 5-HT and its metabolite 5-hydroxyindoleacetic acid (5-HIAA) were also significantly decreased (Figure 2G,H, $P < 0.0001$). Furthermore, the protein and mRNA levels of TPH2 were significantly lower in MS mice than in the control group. However, O-1602 treatment restored the expression of TPH2 in MS mice ($F_{(4,10)} = 83.36$, $P < 0.0001$, Figure 2G,H, $F_{(4,10)} = 85.95$, $P < 0.0001$, Figure 2I). Additionally, 0.1 mg/kg O-1602 treatment had no significant effects on the levels of 5-HT and its metabolite 5-HIAA in the MS mice ($P = 0.8060$), while 0.4 and 2.0 mg/kg of O-1602 significantly increased the levels of 5-HT and its metabolite 5-HIAA ($F_{(4,10)} = 65.51$, $P < 0.0001$, Figure 2J; $F_{(4,10)} = 22.74$, $P < 0.0001$, Figure 2K). Moreover, the protein expression of GPR55 and TPH2 had no significant changes in the DRN of control mice with 0.4 mg/kg O-1602

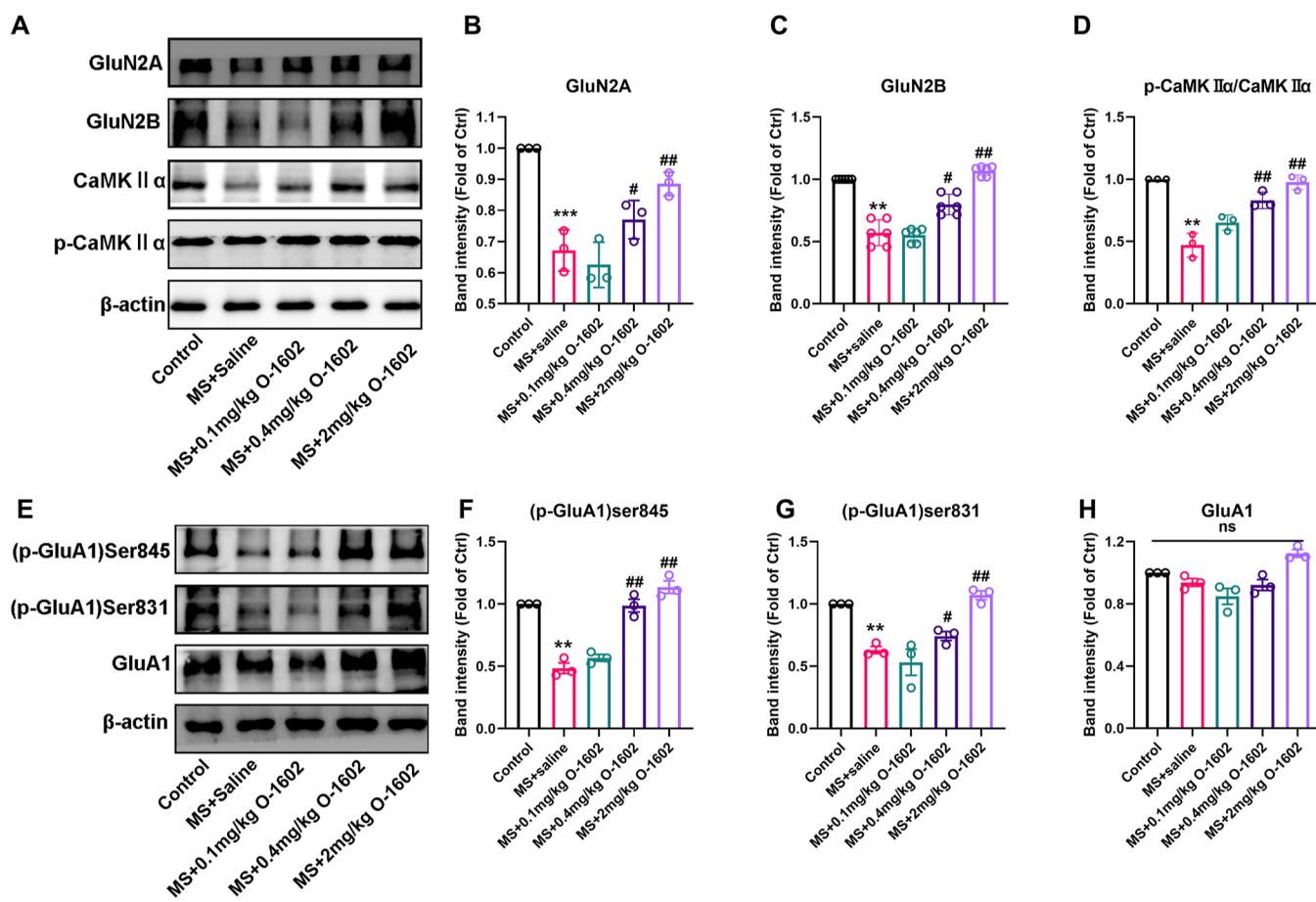


Figure 5. O-1602 upregulated the NMDAR and AMPAR in the MS model. (A–D) Representative western blot images and densitometric analysis of GluN2A, GluN2B, and CaMKII α protein expression in the DRN. The protein expression levels were normalized to beta-actin expression ($n = 3$ mice per group). (E–H) Representative western blot images and densitometric analysis of the phosphorylation of GluR1 at Ser845 (p-GluR1-S845) and Ser831 (p-GluR1-S831), and GluA1 protein expression in the DRN. The protein levels were normalized to beta-actin expression ($n = 3$ mice per group). ns, not significant. All data are shown as mean \pm S.E.M.; ** $p < 0.01$, *** $p < 0.001$ vs control group; # $p < 0.05$, ## $p < 0.01$ vs MS group. ns: no significance.

treatment (Figure S1). These findings indicate that GPR55 activation enhances the expression of TPH2 and promote the synthesis of the 5-HT transmitter in the DRN of MS mice.

2.3. TPH2^{DRN} Knockdown Reduced the Effect of GPR55 Agonist on Learning and Memory in MS Mice. To further clarify whether GPR55 activation specifically affects TPH2 activity and the synthesis of 5-HT in the DRN, thus mitigating learning and memory impairment induced by MS, we injected a TPH2 knockdown adeno-associated virus (AAV) into the DRN of mice. Four weeks (28 days) after microinjections of shTPH2, western blotting analysis showed a knockdown rate of 67% in control mice (6–8 weeks old) (Figure 3B,C, $P < 0.0001$). Furthermore, the levels of 5-HT were significantly decreased after TPH2 knockdown (Figure 3D,E, $P < 0.0001$). Surprisingly, the NORT was initiated on day 29 following AAV injection, and a significant reduction in the discrimination index was detected in the NC (negative control) compared with mice with TPH2^{DRN} knockdown ($F_{(5, 28)} = 8.137$, $P = 0.0022$, Figure 3F). In the MWM test, the NC and mice with TPH2 knockdown showed a decreased frequency of platform crossing, a reduced percentage of time spent in the target quadrant, and an increased latency time ($F_{(5, 30)} = 15.14$, $P < 0.0001$, Figure 3G; $F_{(5, 30)} = 18.54$, $P < 0.0001$, Figure 3H; $F_{(5, 32)} = 7.404$, $P = 0.0001$, Figure 3I). Furthermore, MS mice with TPH2^{DRN} knockdown were administered intraperitoneal injections of O-1602 (0.4 mg/kg)

for five consecutive days, and we found that MS mice with TPH2^{DRN} knockdown significantly weakened the improvement effect of O-1602 on learning and memory impairment, as indicated by the performance in the NORT and MWM test (Figure 3F–I). Our behavioral tests revealed that TPH2 knockdown in the DRN region led to significant cognitive deficits of NC mice and also reduced the beneficial effect of GPR55 activation on learning and memory deficits of MS mice.

2.4. O-1602 Reversed the Reduction of Excitatory Synapse Transmission in the DRN Caused by MS. To gain further insight into the direct influence of GPR55 on 5-HT neurons within the DRN of MS mice, we employed whole-cell patch-clamp recordings to assess alterations in miniature excitatory postsynaptic current (mEPSC). Biocytin was injected into the recorded neurons to verify that the recorded neurons (green) and hm3dq + TPH2 (red) were 5-HT neurons in the DRN (Figure 4A). To determine the role of GPR55 in excitatory synaptic transmission in the DRN, we recorded α -amino-3-hydroxy-5-methyl-4-isoxazolepropionic acid receptor (AMPA)-mediated mEPSCs (Figure 4B). A significant decrease in the mEPSC frequency was detected in MS mice compared with the control animals ($F_{(2, 15)} = 20.17$, $P < 0.0001$, Figure 4C,E). The mEPSC amplitude was also decreased in MS mice compared with the controls ($F_{(2, 15)} = 24.25$, $P < 0.0001$, Figure 4D,F). O-1602 treatment effectively reversed the

decreased mEPSC frequency and amplitude induced by MS (Figure 4C–F). These findings proved that O-1602 directly enhanced excitatory glutamatergic neurotransmission implicated in MS via GPR55 activation.

2.5. O-1602 Upregulated the Expression of the N-Methyl-D-aspartate Receptor (NMDAR) and AMPAR in the DRN of MS Mice. The suppression of glutamatergic transmission by MS could result from the reduced number of glutamate receptors. To test this, we performed western blotting experiment to detect the levels of AMPAR and NMDAR subunits in the DRN from MS, young (6 week-old) male mice. Here, we observed a significant decrease in the expression of GluN2A, GluN2B, and CaMKII α in the MS group compared to the control group in the DRN of juvenile mice (PND 42 \pm 2). However, following treatment with O-1602, the expression of GluN2A, GluN2B, and CaMKII α was notably increased, particularly at doses of 0.4 and 2 mg/kg ($F_{(4, 10)} = 23.89$, $P < 0.0001$, Figure 5A,B; $F_{(4, 25)} = 77.25$, $P < 0.0001$, Figure 5C; $F_{(4, 10)} = 36.15$, $P < 0.0001$, Figure 5D). GluA1 phosphorylation is crucial for AMPAR function and synaptic plasticity.⁴⁵ In the model group, a significant reduction in the phosphorylation levels of GluA1 (Ser 831 and Ser845) was observed compared to the control group ($F_{(4, 10)} = 54.64$, $P < 0.0001$, Figure 5F; $F_{(4, 10)} = 18.98$, $P = 0.0001$, Figure 5G). Treatment with O-1602, however, led to an elevation in these levels, with the most robust effects observed at doses of 0.4 and 2 mg/kg for both Ser831 (Figure 5G, $P = 0.0001$) and Ser845 (Figure 5F, $P < 0.0001$). Additionally, we measured the expression levels of total GluA1 and phosphorylated GluA1. Interestingly, treatment with O-1602 did not affect the levels of total GluA1 compared to the model group with the controls ($F_{(4, 10)} = 10.56$, $P = 0.6694$, Figure 5H). Our research results indicate that O-1602 treatment can upregulate the NMDAR and AMPAR in the DRN. GPR55 may improve MS-induced learning and memory impairment by affecting the postsynaptic NMDAR and AMPAR functions.

3. DISCUSSION

The research findings indicated that MS leads to significant cognitive impairments, particularly in learning and memory. On the one hand, the protein concentrations of GPR55 and TPH2 were reduced in the DRN of MS mice, subsequently impacting the release of 5-HT in the DRN. On the other hand, the excitatory synaptic transmission of 5-HTergic neurons in the DRN of MS mice and the expression of postsynaptic NMDAR- and AMPAR-related proteins are abnormal. However, GPR55 activation promoted the synthesis of TPH2 and release of 5-HT, as well as increase the excitatory synaptic transmission of 5-HTergic neurons and the expression of postsynaptic NMDAR- and AMPAR-related proteins. Understanding the mechanisms by which GPR55 activation influences the expression of TPH2 and these synaptic proteins may lead to the development of therapeutic strategies aimed at mitigating the cognitive deficits observed in MS mice. By restoring 5-HT signaling and promoting synaptic plasticity, these interventions could potentially improve learning and memory processes in mice with MS.

Early adverse life experience during neurodevelopmental periods is a well-recognized risk factor for several psychiatric disorders.^{46,47} One consistent consequence of ELS is cognitive deficits.^{48–50} Previous studies have found that mice subjected to ELS exhibit substantial cognitive impairment in hippocampus-dependent learning and memory tasks, such as the spatial object recognition test, compared to the controls.^{51–54} Therefore, the

ELS animal model has been valuable for investigating treatments targeting cognitive deficits in psychiatric disorders. In this study, we examined the cognitive impairment in MS mice through behavioral tests. Surprisingly, the administration of varying concentrations of the GPR55 agonist O-1602 significantly enhanced the learning and memory of MS mice and restored levels to the ones in control mice. Furthermore, it is worth noting that both medium and high concentrations have a consistent effect on improving MS-induced learning and memory impairment. Additionally, it was observed that the administration of O-1602 in normal mice did not result in any behavioral changes. Based on these findings, we selected the medium dose of O-1602 for further experiments. Coinciding with our results expressed herein, previous studies revealed that GPR55 activation ameliorates cognitive impairment and neurotoxicity in a mouse model of Alzheimer's disease induced by A β 1–42 via inhibiting the Rho subfamily protein A/Rho-related curly junction protein kinase 2 pathway.³⁸ Furthermore, GPR55 activation has been shown to improve the cognitive function of mice by reducing oxidative stress, neuroinflammation, and synaptic impairment.⁵⁵ Therefore, we speculated that GPR55 is a vital receptor affecting cognitive impairment.

5-HTergic neurons in the DRN are essential in early postnatal development, influencing the maturation and modulation of higher-order emotional, sensory, and cognitive circuitry.^{41–43} The DRN located in the midbrain contains most 5-HT neurons projecting to the forebrain, accounting for approximately two-thirds of the total neurons.^{19,44} These 5-HT neurons regulate depression, anxiety, and cognition by projecting to various brain areas, such as the cortex, amygdala, and hippocampus.²⁴ The hippocampus is well-known for their roles in learning and memory in animals. In this study, GPR55 was colabeled with TPH2 in the DRN. The protein expression of GPR55 was significantly downregulated in mice subjected to MS compared to normal mice. However, the decrease in GPR55 expression was reversed by O-1602 treatment. These findings suggest a potential role of GPR55 in the development of learning and memory in the DRN of MS mice. TPH2 is a crucial enzyme involved in the synthesis of 5-HT,⁵⁶ and boosting TPH2 synthesis and enhancing 5-HT release could be potential therapeutic strategies for addressing cognitive impairments.⁵⁷ Previous studies have shown that increased mRNA expression levels of TPH2 can enhance its enzymatic activity, leading to increased 5-HT synthesis.⁵⁸ Our experiments demonstrated that administration of O-1602 increased TPH2 protein concentration and mRNA expression levels, resulting in enhanced 5-HT secretion and significant improvement in learning and memory deficits in mice with MS. To further understand the connection of GPR55 and TPH2 in the DRN, we utilized an AAV to knock down the *TPH2* gene in mice. Behavioral tests revealed that reduced TPH2 levels in the DRN region contributed to significant cognitive deficits of normal mice and also reduced the beneficial effect of GPR55 activation on learning and memory deficits of MS mice. These results suggested that the activation of GPR55 could improve MS-induced learning and memory impairment through facilitating TPH2 synthesis and restoring 5-HT content in the DRN. Additionally, we found that GPR55 activation by O-1602 restored behavior deficits even in TPH2 knockdown mice. This counterintuitive result might be explained as TPH2 short hairpin RNA (shRNA) did not generate a complete knockout, only about 67% knockdown.

Synapses are pivotal in transmitting neuronal impulses, encoding learning and memory and exchanging information.⁵⁹ Synaptic loss is the primary reason for cognitive impairment.^{60,61} Therefore, enhancing synaptic function has emerged as an effective approach to improving learning and memory deficits. MS resulted in a reduction in the frequency and amplitude of mEPSCs of 5-HTergic neurons in the DRN, while treatment with the GPR55 agonist increased both mEPSC frequency and amplitude. Therefore, our experimental results are consistent with the reported studies that both presynaptic and postsynaptic GPR55 are involved in these effects.^{30,62} The plasma glutamate receptors, the NMDAR and AMPAR, are distributed in the postsynaptic density area of excitatory synapses. Activation of these receptors can trigger various forms of synaptic plasticity and facilitate rapid synaptic transmission.⁴⁵ Our data showed that MS significantly downregulated the expression of GluN2A and GluN2B in the DRN, while O-1602 administration restored the levels of both receptors.

The Ca²⁺-CaM-calmodulin-dependent protein kinase II alpha (CaMKII α) signaling pathway, activated by NMDA receptors, plays an essential role in synaptic plasticity, learning, and memory. ELS has a significant impact on the structural and functional plasticity of the hippocampus and prefrontal cortex in adolescents, and the expression of synaptophysin and CaMKII α was decreased.⁶³ Our study showed that the decrease in the expression of p-CaMKII α /CaMKII α in the DRN of the MS group was reversed by O-1602 treatment. Upon activation of NMDA receptors, calcium ions enter cells, activating calcium ion/CaMKII. This process involves direct phosphorylation of various subunits of AMPARs, particularly the phosphorylation of Ser 831 at the carboxyl terminal of the GluA1 subunit, which is critical for the induction and maintenance of long-term potentiation.⁶⁴ The expression of the AMPAR GluA1R did not differ. However, the phosphorylation levels of Ser 845 and Ser 831 of GluA1R were significantly changed in the MS and O-1602 groups. These results suggest that GPR55 reduces excitatory postsynaptic currents by mediating the phosphorylation of AMPARs.

Our study establishes a clear link between diminished GPR55 expression in the DRN and the learning and memory deficits observed in MS conditions. Strikingly, activation of the GPR55 pathway seems to counteract these negative consequences in young adulthood. Additionally, the activation of GPR55 appears to modulate *TPH2* gene expression and related protein expression of the NMDAR and AMPAR, offering therapeutic potential in mitigating the cognitive deficits induced by MS. This work uncovers a previously unidentified role of GPR55 within the central nervous system and sheds light on the intricate molecular underpinnings of learning and memory disturbances in the context of MS. Undoubtedly, this work has certain limitations. First, the present study is limited by the fact that the experiments were only done with male mice. Second, the pentahydroxy tryptamine neurons have been found to project numerous nerve fibers throughout the entire brain and play a significant role in various brain regions.^{44,65} Third, the administration of O-1602 intraperitoneally may affect other brain regions highly associated with learning and memory. In future research, we aim to explore the depth relationship between 5-HTergic neurons in the DRN and learning and memory in the male and female mice, as well as the projection of 5-HTergic neurons to other brain regions in MS, with the goal of generating novel treatment approaches for this disease.

4. MATERIALS AND METHODS

4.1. Animals and Drugs. Pregnant C57BL/6 female mice, pregnancy period of 18–19 days, were purchased from the Air Force Medical University Experimental Animal Center (Xi'an, China) and housed individually in a temperature- and humidity-controlled environment, with a 12:12 h light/dark cycle (light on at 07:00 a.m.) and ad libitum access to food and water. All behavioral tests were performed during the light period on the designated day of the experiment. All experimental procedures were approved by the Air Force Medical University Animal Care and Use Committee (no. 20230702). Efforts were made to reduce the number of animals used and their suffering. O-1602 (purity >98%) was purchased from Tocris Bioscience (Bristol, UK) and dissolved in saline. According to our previous studies,⁶⁶ the doses of O-1602 (0.1, 0.4, and 2.0 mg/kg, once a day) were administered via intraperitoneal injection.

4.2. Establishment of an MS Model. Each pregnant female mouse was checked for delivery twice daily (10:00 a.m. and 07:00 p.m.), and the birth day was designated as PND 0. Then, all pups were randomly assigned to two groups: the control group and the MS group. In the control group, pups and their dams remained undisturbed except for biweekly cage cleaning until weaning. In the MS group, mouse pups were separated from their mothers daily for 3 h (from 9:00 a.m. to 12:00 a.m.) between PNDs 5 and 21. During this time, they were placed in an empty cage with similar temperature and humidity conditions. At the weaning day on PND 22, all litters were separated based on sex and treatment conditions and were maintained in group-housing systems. Only male mice ($n = 6$) were maintained to perform a series of behavioral tests during the juvenile period (PND 42–56). The timeline of the experiment is shown in Figure 1.

4.3. NORT. The NORT was employed to evaluate mice's recognition memory. The NORT was performed as described previously with minor modifications.⁶⁷ This assessment encompasses three sequential stages: habituation, training, and testing. During the initial two-day habituation phase, mice were introduced to an opaque square enclosure with dimensions of 40 × 40 × 25 cm. Without any objects, mice were allowed to explore freely for 10 min to adapt to the environment. On the subsequent training day, the mice were positioned within the enclosure and permitted to investigate two identical objects for 10 min. The next day marked the testing phase, wherein the mice were exposed to two disparate objects for 5 min. One was a familiar object, and the other was novel. A mouse's behavior was categorized as 'exploratory' when it oriented its snout toward an object, maintaining a proximity of approximately 2 cm. To ensure unbiased observations, two independent researchers, uninformed about the experimental groups, meticulously documented the duration each mouse dedicated to exploring the objects. The RI was subsequently derived by taking the ratio of time devoted to the novel object to the cumulative time spent examining both entities.

4.4. MWM Test. The MWM test was used to evaluate the cognitive capability of mice in terms of their learning and memory abilities over five consecutive days. A circular pool measuring 120 cm in diameter was used, surrounded by blue curtains. The pool was divided into four quadrants: I, II, III, and IV. It contained water filled to a depth of 45 cm, which was consistently maintained at 25 ± 1 °C. A platform measuring 6 cm in diameter was placed within one of the quadrants, located 2 cm below the water's surface, to remain hidden from the mice.

The first 4 days were the learning phase. Mice were randomly placed in one of the four quadrants without the platform present. Each mouse underwent four trials on each training day at intertrial intervals of 30–40 min. On the fifth day, the platform was removed. Mice underwent a probe trial, during which they were allowed 60 s of free swimming. The movement paths in this trial were captured by a digital camera and subsequently analyzed using the ANY-maze behavioral tracking software (Stoelting Co., Illinois, USA). The following parameters were measured: escape latency (latency to find the platform) during each training session, the percentage of time spent in the target quadrant during the probe trial, and the number of times the mouse crossed the platform.

4.5. Y-Maze Test. The Y-maze test was performed to evaluate the discriminatory and spatial working memory of mice. The Y maze consisted of three arms designated A, B, and C, arranged at 120° intervals. The ANY-maze animal behavior analysis system was used to record the movements of mice within the Y maze. Mice were placed in the central junction area of the Y maze and allowed to freely explore for 8 min. A complete entry of a mouse's hind limb into any arm was considered an entry into that respective arm. Alternation was defined as the sequential entry of an animal into three different arms (e.g., ABC, ACB, BAC, BCA, CAB, and CBA). The percentage of spontaneous alternation was calculated using the following formula: spontaneous alternation (%) = (successive triplet sets/total number of arm entries - 2) × 100. A higher correct alternation rate indicated stronger spatial discrimination and memory capabilities.

4.6. Immunofluorescence Staining. After completing behavior tests, mice from the control and MS groups ($n = 6$ per group, 7–8 weeks old) were anesthetized with pentobarbital sodium. Subsequently, they were intracardially perfused with sterile saline, followed by 4% paraformaldehyde in 0.1 M PBS (pH 7.4). The brain was postfixed in 4% paraformaldehyde overnight and dehydrated through an ascending sucrose series, including 15 and 30% (w/v) sucrose in 0.1 M PBS at 4 °C overnight. Subsequently, floating sections (25 μm) of the DRN were obtained and subjected to immunohistochemistry staining using anti-GPR55 (Abcam, ab203663; 1:200) and anti-TPH2 (Abcam, ab133477; 1:200) antibodies. After washing three times, sections were incubated with secondary antibodies diluted in PBST for 2 h at room temperature in the dark. DAPI diluted in 0.1 M PBS (1:1000) was applied to mark cell nuclei. A confocal fluorescence microscopy (Olympus, Japan) was employed to observe and acquire the images. Image analysis and process were carried out using ImageJ (NIH) by researchers blinded to the experiments.

4.7. Western Blotting. Western blotting was performed as previously described.⁶⁸ After completing behavior tests, mice were euthanized in the control, MS, and O-1602 treatment groups ($n = 3$ per group, 7–8 weeks old). Subsequently, their brains were removed and sliced, and the DRN was carefully excised under a microscope. Total protein was extracted from DRN samples using the M-PER protein extraction buffer. Protein concentration was determined using a BCA kit. Equal amounts of protein samples were used for western blotting analysis. The primary antibodies used in this experiment were as follows: GPR55 (Abcam, ab203663; 1:1000), GluN2A (Abcam, ab124913; 1:1000), GluN2B (Abcam, ab254356; 1:1000), *p*-CaMKII α (Abcam, ab171095; 1:1000), CaMKII α (Abcam, ab52476; 1:1000), *p*-GluA1R Ser831 (Abcam, ab109464; 1:1000), *p*-GluA1R Ser45 (Abcam, ab76321; 1:1000), GluA1

(Abcam, ab31232; 1:1000), and TPH2 (Abcam, ab133477; 1:1000). β -Actin (Sigma-Aldrich, A5316; 1:10,000) was used as a loading control. After three washes with TBST for 10 min, the membranes were incubated with horseradish peroxidase-conjugated secondary antibodies. Then, the signal of the target protein was detected and digitized using the ECL solution and the ImageJ program. The band intensity of each blot was quantified as a ratio relative to β -actin. And we normalized all the data to obtain the same value in the control group.

4.8. Viral Injection. Mice from control and MS groups (6–8 weeks old) were administered sodium pentobarbital (50 mg kg⁻¹, i.p. injection) for bilateral stereotaxic injection of viruses. The mice were microinjected in the DRN (anteroposterior (AP) -4.7 mm, dorsoventral (DV) -3.3 mm) with a total 200 nL of viral cocktail (1:1) of rAAV-TPH2-CRE-P2A-EGFP-WPREs and rAAV-Efla-DIO-hM3D(Gq)-mCherry-WPREs (Brain-VTA, Wuhan, China) to facilitate the initial infection of 5-HT neurons. Four weeks after the transfection and expression of the chemogenetic virus in the DRN of mice, behavioral tests were conducted at 2.5 h following an injection of 1 mg/kg clozapine-N-oxide.

4.9. Whole-Cell Patch-Clamp Recordings. In voltage clamp mode, currents were recorded at a holding potential of -70 mV using recording pipettes filled with an intracellular solution consisting of 0.2 mM tris-GTP, 0.4 mM EGTA, 4 mM Mg-ATP, 5 mM NaCl, 10 mM HEPES, 20 mM KCl, and 130 mM potassium gluconate (pH 7.2–7.4; osmolality 290–300 mOsm). Spontaneous excitatory postsynaptic currents were recorded from layer I and layer II neurons using an Axon 700B amplifier (Molecular Devices Inc., CA, USA).

Animals from control, MS, and MS + 0.4 mg/kg groups ($n = 6$ per group, 6–8 weeks old) were sacrificed by cervical dislocation. DRN samples (300 μm) were coronally sliced in ice-cold artificial cerebrospinal fluid (ACSF; pH = 7.2–7.4) containing 124 mM NaCl, 2.5 mM KCl, 2 mM CaCl₂, 2 mM MgSO₄, 25 mM NaHCO₃, 1 mM NaH₂PO₄, and 37 mM glucose. The ACSF was saturated with 95% O₂/5% CO₂, followed by 1 h incubation at room temperature, and then DRN brain slices were transferred to the recording chamber on the stage of an Olympus microscope. Voltage-clamp recordings of mEPSCs were conducted in a whole-cell mode ($V_h = -70$ mV) with 100 μM picrotoxin and 1 μM TTX using recording pipettes filled with an intracellular solution consisting of 0.2 mM tris-GTP, 0.4 mM EGTA, 4 mM Mg-ATP, 5 mM NaCl, 10 mM HEPES, 20 mM KCl, and 130 mM potassium gluconate (pH 7.2–7.4; osmolality 290–300 mOsm). All signals from neurons were obtained and recorded using a Multi Clamp 700B Amplifier (Axon Instruments, Foster City, CA, USA). Data were excluded if the access resistance changed by more than 15% during the experiment or if the resting membrane potential was more depolarized than -70 mV. Offline analysis of voltage clamp data was performed using the Mini Analysis Program 6.0.7.

To identify the morphological properties of the recorded neurons, biocytin (0.5%) was applied to the pipet solution. After finishing data recording, the brain slices were fixed and stored as mentioned above in the Immunofluorescence Staining section.

4.10. shRNA AAV Construction and Transfection. To knock down TPH2 (NM_173391.3), plasmids encoding shRNA targeting TPH2 were designed using validated shRNA sequences: 5'-ATGTGGCCATGGGCTATAAAT-3'. The AAV vector was generated by inserting shRNA fragments into

the AAV vector GV478. A NC shRNA was used as an AAV infection control.

4.11. Stereotaxic Surgery and Microinjections. Mice in the control and MS groups ($n = 6$ per group, 6–8 weeks old) were anesthetized using a mixture of ketamine (30 mg/mL) and xylazine (3 mg/mL) and then mounted onto a stereotaxic apparatus (RWD68001, Shenzhen Ruiwode Life Science, China). An attenuated glass electrode with a diameter of approximately 10 μm was bilaterally implanted into the DRN (−4.7 mm AP and −3.3 mm DV). Microinjections of 200 nL of shTPH2 (2.49×10^{12} v.g./mL) were administered bilaterally at a rate of 40 nL/min using an infusion pump (Harvard Apparatus, MA). An AAV vector containing 200 nL of NC was used as an infection control. Four weeks after the shRNA infection, mice were treated with O-1602 for 5 days. All groups (NC, MS, shTPH2, and shTPH2 + MS + O-1602 groups) of mice were subjected to behavioral tests at 10–14 weeks.

4.12. ELISA. Brain atlas coordinates and brain localization were utilized in this study. DRN tissues were extracted from the mice ($n = 5$ per group, 7–8 weeks old) brains in the control, MS, and O-1602 treatment groups under a microscope. Subsequently, the tissues were rinsed with precooled PBS (0.01 M, pH 7.4) to remove residual blood. The tissue was then weighed and cut into smaller pieces. These shredded tissue fragments were combined with an appropriate volume of PBS (typically in a 1:9 weight to volume ratio) in a glass homogenizer, with protease inhibitors added to the PBS. The mixture was thoroughly ground on ice to ensure complete homogenization. Following the manufacturer's instructions, the microwell coated with mouse 5-HT and 5-HIAA trapping antibody was added with specimens, the standard, and a horseradish peroxidase-labeled detection antibody successively, warmed, and thoroughly washed. Color development was achieved using the substrate TMB, initially converting to blue through peroxidase catalysis and then to yellow in response to acid. The color intensity was proportional to the concentration of the mouse interleukin-1 β in the sample. Absorbance (OD value) was measured at a wavelength of 450 nm using an enzyme-labeled instrument, and the sample concentration was calculated.

4.13. RNA Extraction and Quantitative Real-Time PCR (qRT-PCR). After behavior tests, total RNA was extracted from DRN brain tissues of control, MS, and O-1602 treatment groups ($n = 3$ per group, 7–8 weeks old) using standard phenol/chloroform extraction method. The One Step SYBR Prime-Script RT-PCR Kit was used for cDNA synthesis according to the manufacturer's protocols. qRT-PCR was performed using SYBR Premix ExTaq on a Bio-Rad CFX96TM Real-Time PCR Detection System (Bio-Rad) with the following thermocycling conditions: 95 °C denaturation for 15 min, followed by 40 cycles of denaturation at 95 °C for 10 s, and annealing at 55 °C for 30 s. The fluorescent product was detected at the end of 95 °C extension incubation. Melting curve analysis was then performed on PCR products, and the relative expression of each gene was calculated using the $2^{-\Delta\Delta\text{CT}}$ method. All qRT-PCR reactions were performed in triplicate, and the expression of the target gene was normalized to the mRNA level of *GAPDH*. The primers for *TPH2* (forward: 5'-CCCAAGTTCGCTCAGTTTTC-3'; reverse: 5'-CACACGCCTGTCCAGAAAGA-3') and *GAPDH* (forward: 5'-CATGCTTCCGTGTTCTTA-3'; reverse: 5'-CTTACCA-CCTTCTTGATGTCATC-3') were provided by Sangon Biotech (Shanghai, China).

4.14. Statistical Analysis. All data were expressed as mean \pm S.E.M. Statistical comparisons were performed using GraphPad Prism 8.0 (GraphPad Software) with appropriate methods specified in the figure legends. Multigroup comparisons were conducted using one-way analysis of variance (ANOVA) followed by Tukey's test or two-way ANOVA followed by Bonferroni's test. A significance level of $p < 0.05$ was considered statistically significant.

■ ASSOCIATED CONTENT

Supporting Information

The Supporting Information is available free of charge at <https://pubs.acs.org/doi/10.1021/acsomega.3c08934>.

Representative western blot images and densitometric analysis of GPR55 and TPH2 protein expression in the DRN (PDF)

■ AUTHOR INFORMATION

Corresponding Authors

Ming-Gao Zhao – Precision Pharmacy & Drug Development Center, Department of Pharmacy, The Second Affiliated Hospital of Air Force Medical University, Xi'an 710038, China; orcid.org/0000-0002-7539-3887; Email: yangqifmmu@126.com

Qi Yang – Precision Pharmacy & Drug Development Center, Department of Pharmacy, The Second Affiliated Hospital of Air Force Medical University, Xi'an 710038, China; Phone: 86-29-84777164; Email: minggao@fmmu.edu.cn; Fax: 86-29-84777164

Authors

Ting Sun – Precision Pharmacy & Drug Development Center, Department of Pharmacy, The Second Affiliated Hospital of Air Force Medical University, Xi'an 710038, China

Ya-Ya Du – Precision Pharmacy & Drug Development Center, Department of Pharmacy, The Second Affiliated Hospital of Air Force Medical University, Xi'an 710038, China

Yong-Qiang Zhang – Department of Chinese Materia Medica and Natural Medicines, School of Pharmacy, Air Force Medical University, Xi'an 710032, China

Qin-Qin Tian – Department of Chemistry, School of Pharmacy, Air Force Medical University, Xi'an 710032, China

Xi Li – Precision Pharmacy & Drug Development Center, Department of Pharmacy, The Second Affiliated Hospital of Air Force Medical University, Xi'an 710038, China

Jiao-Yan Yu – Precision Pharmacy & Drug Development Center, Department of Pharmacy, The Second Affiliated Hospital of Air Force Medical University, Xi'an 710038, China

Yan-Yan Guo – Precision Pharmacy & Drug Development Center, Department of Pharmacy, The Second Affiliated Hospital of Air Force Medical University, Xi'an 710038, China

Qing-Qing Liu – Precision Pharmacy & Drug Development Center, Department of Pharmacy, The Second Affiliated Hospital of Air Force Medical University, Xi'an 710038, China

Le Yang – Precision Pharmacy & Drug Development Center, Department of Pharmacy, The Second Affiliated Hospital of Air Force Medical University, Xi'an 710038, China; orcid.org/0009-0003-1688-1383

Yu-Mei Wu – Department of Pharmacology, School of Pharmacy, Air Force Medical University, Xi'an 710032, China; orcid.org/0000-0002-8524-1254

Complete contact information is available at:

<https://pubs.acs.org/10.1021/acsomega.3c08934>

Author Contributions

T.S., Y.-Y.D., and Y.-Q.Z. contributed equally to this study. T.S., Y.-Q.Z., and M.-G.Z. designed the study. Y.-Y.D., Q.-Q.T., Y.-Q.Z., and Q.-Q.L. carried out the experiments, and X.L. and Y.-Y.G. analyzed the data. T.S., L.Y., and Y.-M.W. drafted the manuscript and verified the important intellectual content. All authors critically read and revised the manuscript and approved the final version of the manuscript for submission.

Notes

The authors declare no competing financial interest.

ACKNOWLEDGMENTS

This work was supported in part by research grants from the National Natural Science Foundation of China (no. 81801079 to T.S., no. 81870893 to Q.Y., and no. 82071515 to Y.M.W.) and from the National Postdoctoral Program for Innovative Talents (no. BX20160025 to Q.Y.). The funding sources played no role in the study design, the collection, analysis, and interpretation of data, in the writing of the report, and in the decision to submit the article for publication.

REFERENCES

- (1) Bale, T. L.; Baram, T. Z.; Brown, A. S.; Goldstein, J. M.; Insel, T. R.; McCarthy, M. M.; Nemeroff, C. B.; Reyes, T. M.; Simerly, R. B.; Susser, E. S.; Nestler, E. J. Early life programming and neurodevelopmental disorders. *Biol. Psychiatry* **2010**, *68* (4), 314–319.
- (2) Pechtel, P.; Pizzagalli, D. A. Effects of early life stress on cognitive and affective function: an integrated review of human literature. *Psychopharmacology* **2011**, *214* (1), 55–70.
- (3) Lemaire, V.; Koehl, M.; Le Moal, M.; Abrous, D. N. Prenatal stress produces learning deficits associated with an inhibition of neurogenesis in the hippocampus. *Proc. Natl. Acad. Sci. U.S.A.* **2000**, *97* (20), 11032–11037.
- (4) Heim, C.; Nemeroff, C. B. The role of childhood trauma in the neurobiology of mood and anxiety disorders: preclinical and clinical studies. *Biol. Psychiatry* **2001**, *49* (12), 1023–1039.
- (5) Morgan, C.; Fisher, H. Environment and schizophrenia: environmental factors in schizophrenia: childhood trauma—a critical review. *Schizophr. Bull.* **2006**, *33* (1), 3–10.
- (6) Talge, N. M.; Neal, C.; Glover, V. Antenatal maternal stress and long-term effects on child neurodevelopment: how and why? *J. Child Psychol. Psychiatry* **2007**, *48* (3–4), 245–261.
- (7) Bremner, J. D.; Vermetten, E. Stress and development: behavioral and biological consequences. *Dev. Psychopathol.* **2001**, *13* (3), 473–489.
- (8) Fatemi, S. H.; Folsom, T. D. The neurodevelopmental hypothesis of schizophrenia, revisited. *Schizophr. Bull.* **2009**, *35* (3), 528–548.
- (9) Teicher, M. H.; Andersen, S. L.; Polcari, A.; Anderson, C. M.; Navalta, C. P.; Kim, D. M. The neurobiological consequences of early stress and childhood maltreatment. *Neurosci. Biobehav. Rev.* **2003**, *27* (1–2), 33–44.
- (10) Cirulli, F.; Francia, N.; Berry, A.; Aloe, L.; Alleva, E.; Suomi, S. J. Early life stress as a risk factor for mental health: role of neurotrophins from rodents to non-human primates. *Neurosci. Biobehav. Rev.* **2009**, *33* (4), 573–585.
- (11) Ellenbroek, B. A.; Derks, N.; Park, H.-J. Early maternal deprivation retards neurodevelopment in Wistar rats. *Stress* **2005**, *8* (4), 247–257.
- (12) Lehmann, J.; Russig, H.; Feldon, J.; Pryce, C. R. Effect of a single maternal separation at different pup ages on the corticosterone stress response in adult and aged rats. *Pharmacol., Biochem. Behav.* **2002**, *73* (1), 141–145.
- (13) Rentesi, G.; Antoniou, K.; Marselos, M.; Fotopoulos, A.; Alboycharali, J.; Konstandi, M. Long-term consequences of early maternal deprivation in serotonergic activity and HPA function in adult rat. *Neurosci. Lett.* **2010**, *480* (1), 7–11.
- (14) Llorente, R.; Miguel-Blanco, C.; Aisa, B.; Lachize, S.; Borcel, E.; Meijer, O. C.; Ramirez, M. J.; De Kloet, E. R.; Viveros, M. P. Long term sex-dependent psychoneuroendocrine effects of maternal deprivation and juvenile unpredictable stress in rats. *J. Neuroendocrinol.* **2011**, *23* (4), 329–344.
- (15) Llorente, R.; O’Shea, E.; Gutierrez-Lopez, M. D.; Llorente-Berzal, A.; Colado, M. I.; Viveros, M.-P. Sex-dependent maternal deprivation effects on brain monoamine content in adolescent rats. *Neurosci. Lett.* **2010**, *479* (2), 112–117.
- (16) Llorente, R.; Villa, P.; Marco, E. M.; Viveros, M. P. Analyzing the effects of a single episode of neonatal maternal deprivation on metabolite profiles in rat brain: a proton nuclear magnetic resonance spectroscopy study. *Neuroscience* **2012**, *201*, 12–19.
- (17) Roceri, M.; Hendriks, W.; Racagni, G.; Ellenbroek, B. A.; Riva, M. A. Early maternal deprivation reduces the expression of BDNF and NMDA receptor subunits in rat hippocampus. *Mol. Psychiatry* **2002**, *7* (6), 609–616.
- (18) Lesch, K.-P.; Waider, J. Serotonin in the modulation of neural plasticity and networks: implications for neurodevelopmental disorders. *Neuron* **2012**, *76* (1), 175–191.
- (19) Zhang, X.; Beaulieu, J.-M.; Sotnikova, T. D.; Gainetdinov, R. R.; Caron, M. G. Tryptophan hydroxylase-2 controls brain serotonin synthesis. *Science* **2004**, *305* (5681), 217.
- (20) van der Veen, F. M.; Evers, E. A. T.; van Deursen, J. A.; Deutz, N. E. P.; Backes, W. H.; Schmitt, J. A. J. Acute tryptophan depletion reduces activation in the right hippocampus during encoding in an episodic memory task. *Neuroimage* **2006**, *31* (3), 1188–1196.
- (21) Karakuyu, D.; Herold, C.; Güntürkün, O.; Diekamp, B. Differential increase of extracellular dopamine and serotonin in the ‘prefrontal cortex’ and striatum of pigeons during working memory. *Eur. J. Neurosci.* **2007**, *26* (8), 2293–2302.
- (22) Chamas, F.; Serova, L.; Sabban, E. L. Tryptophan hydroxylase mRNA levels are elevated by repeated immobilization stress in rat raphe nuclei but not in pineal gland. *Neurosci. Lett.* **1999**, *267* (3), 157–160.
- (23) Kim, S. W.; Park, S. Y.; Hwang, O. Up-regulation of tryptophan hydroxylase expression and serotonin synthesis by sertraline. *Mol. Pharmacol.* **2002**, *61* (4), 778–785.
- (24) Lesch, K.-P.; Araragi, N.; Waider, J.; van den Hove, D.; Gutknecht, L. Targeting brain serotonin synthesis: insights into neurodevelopmental disorders with long-term outcomes related to negative emotionality, aggression and antisocial behaviour. *Philos. Trans. R. Soc. London, Ser. B* **2012**, *367* (1601), 2426–2443.
- (25) Poleszak, E.; Wośko, S.; Sławińska, K.; Wyska, E.; Szopa, A.; Doboszewska, U.; Właz, P.; Właz, A.; Dudka, J.; Szponar, J.; Serefko, A. Influence of the CB1 cannabinoid receptors on the activity of the monoaminergic system in the behavioural tests in mice. *Brain Res. Bull.* **2019**, *150*, 179–185.
- (26) Zimmermann, T.; Maroso, M.; Beer, A.; Baddenhausen, S.; Ludewig, S.; Fan, W.; Vennin, C.; Loch, S.; Berninger, B.; Hofmann, C.; Korte, M.; Soltesz, I.; Lutz, B.; Leschik, J. Neural stem cell lineage-specific cannabinoid type-1 receptor regulates neurogenesis and plasticity in the adult mouse hippocampus. *Cereb. Cortex* **2018**, *28* (12), 4454–4471.
- (27) Shen, C.-J.; Zheng, D.; Li, K.-X.; Yang, J.-M.; Pan, H.-Q.; Yu, X.-D.; Fu, J.-Y.; Zhu, Y.; Sun, Q.-X.; Tang, M.-Y.; Zhang, Y.; Sun, P.; Xie, Y.; Duan, S.; Hu, H.; Li, X.-M. Cannabinoid CB1 receptors in the amygdalar cholecystokinin glutamatergic afferents to nucleus accumbens modulate depressive-like behavior. *Nat. Med.* **2019**, *25* (2), 337–349.
- (28) Zhang, H.; Li, L.; Sun, Y.; Zhang, X.; Zhang, Y.; Xu, S.; Zhao, P.; Liu, T. Sevoflurane prevents stroke-induced depressive and anxiety behaviors by promoting cannabinoid receptor subtype I-dependent interaction between β -arrestin 2 and extracellular signal-regulated kinases 1/2 in the rat hippocampus. *J. Neurochem.* **2016**, *137* (4), 618–629.
- (29) Liu, B.; Song, S.; Jones, P. M.; Persaud, S. J. GPR55: from orphan to metabolic regulator? *Pharmacol. Ther.* **2015**, *145*, 35–42.

- (30) Sylantyev, S.; Jensen, T.; Ross, R.; Rusakov, D. Cannabinoid- and lysophosphatidylinositol-sensitive receptor GPR55 boosts neurotransmitter release at central synapses. *Proc. Natl. Acad. Sci. U.S.A.* **2013**, *110*, 5193–5198.
- (31) Celorrio, M.; Rojo-Bustamante, E.; Fernandez-Suarez, D.; Saez, E.; Estella-Hermoso de Mendoza, A.; Muller, C. E.; Ramirez, M. J.; Oyarzabal, J.; Franco, R.; Aymerich, M. S. GPR55: A therapeutic target for Parkinson's disease? *Neuropharmacology* **2017**, *125*, 319–332.
- (32) Kallendrusch, S.; Kremzow, S.; Nowicki, M.; Grabiec, U.; Winkelmann, R.; Benz, A.; Kraft, R.; Bechmann, I.; Dehghani, F.; Koch, M. The G Protein-Coupled Receptor 55 Ligand 1- α -Lysophosphatidylinositol Exerts Microglia-Dependent Neuroprotection After Excitotoxic Lesion. *Glia* **2013**, *61* (11), 1822–1831.
- (33) Rahimi, A.; Hajizadeh Moghaddam, A.; Roohbakhsh, A. Central administration of GPR55 receptor agonist and antagonist modulates anxiety-related behaviors in rats. *Fundam. Clin. Pharmacol.* **2015**, *29* (2), 185–1890.
- (34) Deliu, E.; Sperow, M.; Console-Bram, L.; Carter, R. L.; Tilley, D. G.; Kalamarides, D. J.; Kirby, L. G.; Brailoiu, G. C.; Brailoiu, E.; Benamar, K.; Abood, M. E. The Lysophosphatidylinositol Receptor GPR55 Modulates Pain Perception in the Periaqueductal Gray. *Mol. Pharmacol.* **2015**, *88* (2), 265–272.
- (35) Cherif, H.; Argaw, A.; Cecyre, B.; Bouchard, A.; Gagnon, J.; Javadi, P.; Desgent, S.; Mackie, K.; Bouchard, J.-F. Role of GPR55 during Axon Growth and Target Innervation. *eNeuro* **2015**, *2* (5), No. ENEURO.0011-15.2015.
- (36) Guy, A. T.; Nagatsuka, Y.; Ooashi, N.; Inoue, M.; Nakata, A.; Greimel, P.; Inoue, A.; Nabetani, T.; Murayama, A.; Ohta, K.; Ito, Y.; Aoki, J.; Hirabayashi, Y.; Kamiguchi, H. Glycerophospholipid regulation of modality-specific sensory axon guidance in the spinal cord. *Science* **2015**, *349* (6251), 974–977.
- (37) Vong, C. T.; Tseng, H. H. L.; Kwan, Y. W.; Lee, S. M.-Y.; Hoi, M. P. M. Novel protective effect of O-1602 and abnormal cannabidiol, GPR55 agonists, on ER stress-induced apoptosis in pancreatic β -cells. *Biomed. Pharmacother.* **2019**, *111*, 1176–1186.
- (38) Xiang, X.; Wang, X.; Jin, S.; Hu, J.; Wu, Y.; Li, Y.; Wu, X. Activation of GPR55 attenuates cognitive impairment and neurotoxicity in a mouse model of Alzheimer's disease induced by $A\beta$ 1–42 through inhibiting RhoA/ROCK2 pathway. *Prog. Neuro-Psychopharmacol. Biol. Psychiatry* **2022**, *112*, 110423.
- (39) Pérez-Olives, C.; Rivas-Santisteban, R.; Lillo, J.; Navarro, G.; Franco, R. Recent Advances in the Potential of Cannabinoids for Neuroprotection in Alzheimer's, Parkinson's, and Huntington's Diseases. *Adv. Exp. Med. Biol.* **2021**, *1264*, 81–92.
- (40) Sánchez-Zavaleta, R.; Avalos-Fuentes, J. A.; González-Hernández, A. V.; Recillas-Morales, S.; Paz-Bermúdez, F. J.; Leyva-Gómez, G.; Cortés, H.; Florán, B. Presynaptic nigral GPR55 receptors stimulate [3 H]-GABA release through [3 H]-cAMP production and PKA activation and promote motor behavior. *Synapse* **2022**, *76* (11–12), No. e22246.
- (41) Gaspar, P.; Cases, O.; Maroteaux, L. The developmental role of serotonin: news from mouse molecular genetics. *Nat. Rev. Neurosci.* **2003**, *4* (12), 1002–1012.
- (42) Brummelte, S.; Mc Glanaghy, E.; Bonnin, A.; Oberlander, T. F. Developmental changes in serotonin signaling: Implications for early brain function, behavior and adaptation. *Neuroscience* **2017**, *342*, 212–231.
- (43) Fossat, P.; Bacqué-Cazenave, J.; De Deurwaerdère, P.; Cattaert, D.; Delbecq, J.-P. Serotonin, but not dopamine, controls the stress response and anxiety-like behavior in the crayfish *Procambarus clarkii*. *J. Exp. Biol.* **2015**, *218* (Pt 17), 2745–2752.
- (44) Yu, X.-D.; Zhu, Y.; Sun, Q.-X.; Deng, F.; Wan, J.; Zheng, D.; Gong, W.; Xie, S.-Z.; Shen, C.-J.; Fu, J.-Y.; Huang, H.; Lai, H.-Y.; Jin, J.; Li, Y.; Li, X.-M. Distinct serotonergic pathways to the amygdala underlie separate behavioral features of anxiety. *Nat. Neurosci.* **2022**, *25* (12), 1651–1663.
- (45) Shi, S.-H.; Cheng, T.; Jan, L. Y.; Jan, Y.-N. The immunoglobulin family member dendrite arborization and synapse maturation 1 (Dasm1) controls excitatory synapse maturation. *Proc. Natl. Acad. Sci. U.S.A.* **2004**, *101* (36), 13346–13351.
- (46) Short, A. K.; Baram, T. Z. Early-life adversity and neurological disease: age-old questions and novel answers. *Nat. Rev. Neurol.* **2019**, *15* (11), 657–669.
- (47) LeMoult, J.; Humphreys, K. L.; Tracy, A.; Hoffmeister, J.-A.; Ip, E.; Gotlib, I. H. Meta-analysis: Exposure to Early Life Stress and Risk for Depression in Childhood and Adolescence. *J. Am. Acad. Child Adolesc. Psychiatry* **2020**, *59* (7), 842–855.
- (48) Chakrabarty, T.; Harkness, K. L.; McInerney, S. J.; Quilty, L. C.; Milev, R. V.; Kennedy, S. H.; Frey, B. N.; MacQueen, G. M.; Müller, D. J.; Rotzinger, S.; Uher, R.; Lam, R. W. Childhood maltreatment and cognitive functioning in patients with major depressive disorder: a CAN-BIND-1 report. *Psychol. Med.* **2020**, *50* (15), 2536–2547.
- (49) Ganguly, P.; Holland, F. H.; Brenhouse, H. C. Functional Uncoupling NMDAR NR2A Subunit from PSD-95 in the Prefrontal Cortex: Effects on Behavioral Dysfunction and Parvalbumin Loss after Early-Life Stress. *Neuropsychopharmacology* **2015**, *40* (12), 2666–2675.
- (50) Yang, X.-D.; Liao, X.-M.; Uribe-Mariño, A.; Liu, R.; Xie, X.-M.; Jia, J.; Su, Y.-A.; Li, J.-T.; Schmidt, M. V.; Wang, X.-D.; Si, T.-M. Stress during a critical postnatal period induces region-specific structural abnormalities and dysfunction of the prefrontal cortex via CRF1. *Neuropsychopharmacology* **2015**, *40* (5), 1203–1215.
- (51) Wang, X.-D.; Rammes, G.; Kraev, I.; Wolf, M.; Lieb, C.; Scharf, S. H.; Rice, C. J.; Wurst, W.; Holsboer, F.; Deussing, J. M.; Baram, T. Z.; Stewart, M. G.; Müller, M. B.; Schmidt, M. V. Forebrain CRF₁ modulates early-life stress-programmed cognitive deficits. *J. Neurosci.* **2011**, *31* (38), 13625–13634.
- (52) Pillai, A. G.; Arp, M.; Velzing, E.; Lesuis, S. L.; Schmidt, M. V.; Holsboer, F.; Joëls, M.; Krugers, H. J. Early life stress determines the effects of glucocorticoids and stress on hippocampal function: Electrophysiological and behavioral evidence respectively. *Neuropharmacology* **2018**, *133*, 307–318.
- (53) Shin, S.; Lee, S. The impact of environmental factors during maternal separation on the behaviors of adolescent C57BL/6 mice. *Front. Mol. Neurosci.* **2023**, *16*, 1147951.
- (54) Talani, G.; Biggio, F.; Gorule, A. A.; Licheri, V.; Saolini, E.; Colombo, D.; Sarigu, G.; Petrella, M.; Vedele, F.; Biggio, G.; Sanna, E. Sex-dependent changes of hippocampal synaptic plasticity and cognitive performance in C57BL/6J mice exposed to neonatal repeated maternal separation. *Neuropharmacology* **2023**, *222*, 109301.
- (55) Xiang, X.; Wang, X.; Wu, Y.; Hu, J.; Li, Y.; Jin, S.; Wu, X. Activation of GPR55 attenuates cognitive impairment, oxidative stress, neuroinflammation, and synaptic dysfunction in a streptozotocin-induced Alzheimer's mouse model. *Pharmacol., Biochem. Behav.* **2022**, *214*, 173340.
- (56) Walther, D. J.; Bader, M. A unique central tryptophan hydroxylase isoform. *Biochem. Pharmacol.* **2003**, *66* (9), 1673–1680.
- (57) Charles, P. D.; Ambigapathy, G.; Geraldine, P.; Akbarsha, M. A.; Rajan, K. E. Bacopa monniera leaf extract up-regulates tryptophan hydroxylase (TPH2) and serotonin transporter (SERT) expression: implications in memory formation. *J. Ethnopharmacol.* **2011**, *134* (1), 55–61.
- (58) Waider, J.; Araragi, N.; Gutknecht, L.; Lesch, K.-P. Tryptophan hydroxylase-2 (TPH2) in disorders of cognitive control and emotion regulation: a perspective. *Psychoneuroendocrinology* **2011**, *36* (3), 393–405.
- (59) McDaid, J.; Mustaly-Kalimi, S.; Stutzmann, G. E. Ca²⁺ Dyshomeostasis Disrupts Neuronal and Synaptic Function in Alzheimer's Disease. *Cells* **2020**, *9* (12), 2655.
- (60) Robinson, J. L.; Molina-Porcel, L.; Corrada, M. M.; Raible, K.; Lee, E. B.; Lee, V. M.-Y.; Kawas, C. H.; Trojanowski, J. Q. Perforant path synaptic loss correlates with cognitive impairment and Alzheimer's disease in the oldest-old. *Brain* **2014**, *137* (9), 2578–2587.
- (61) Loera-Valencia, R.; Cedazo-Minguez, A.; Kenigsberg, P. A.; Page, G.; Duarte, A. I.; Giusti, P.; Zusso, M.; Robert, P.; Frisoni, G. B.; Cattaneo, A.; Zille, M.; Boltze, J.; Cartier, N.; Buee, L.; Johansson, G.; Winblad, B. Current and emerging avenues for Alzheimer's disease drug targets. *J. Intern. Med.* **2019**, *286* (4), 398–437.

(62) Rosenberg, E. C.; Chamberland, S.; Bazelot, M.; Nebet, E. R.; Wang, X.; McKenzie, S.; Jain, S.; Greenhill, S.; Wilson, M.; Marley, N.; Salah, A.; Bailey, S.; Patra, P. H.; Rose, R.; Chenouard, N.; Sun, S. E. D.; Jones, D.; Buzsaki, G.; Devinsky, O.; Woodhall, G.; Scharfman, H. E.; Whalley, B. J.; Tsien, R. W. Cannabidiol modulates excitatory-inhibitory ratio to counter hippocampal hyperactivity. *Neuron* **2023**, *111* (8), 1282–1300.

(63) Hescham, S.; Grace, L.; Kellaway, L. A.; Bugarith, K.; Russell, V. A. Effect of exercise on synaptophysin and calcium/calmodulin-dependent protein kinase levels in prefrontal cortex and hippocampus of a rat model of developmental stress. *Metab. Brain Dis.* **2009**, *24* (4), 701–709.

(64) Lledo, P. M.; Hjelmstad, G. O.; Mukherji, S.; Soderling, T. R.; Malenka, R. C.; Nicoll, R. A. Calcium/calmodulin-dependent kinase II and long-term potentiation enhance synaptic transmission by the same mechanism. *Proc. Natl. Acad. Sci. U.S.A.* **1995**, *92* (24), 11175–11179.

(65) Li, C.; Meng, F.; Garza, J. C.; Liu, J.; Lei, Y.; Kirov, S. A.; Guo, M.; Lu, X. Y. Modulation of depression-related behaviors by adiponectin AdipoR1 receptors in 5-HT neurons. *Mol. Psychiatry* **2021**, *26* (8), 4205–4220.

(66) Liu, Q.; Yu, J.; Li, X.; Guo, Y.; Sun, T.; Luo, L.; Ren, J.; Jiang, W.; Zhang, R.; Yang, P.; Yang, Q. Cannabinoid receptor GPR55 activation blocks nicotine use disorder by regulation of AMPAR phosphorylation. *Psychopharmacology* **2021**, *238* (11), 3335–3346.

(67) Qiu, C.; Wang, M.; Yu, W.; Rong, Z.; Zheng, H.-S.; Sun, T.; Liu, S.-B.; Zhao, M.-G.; Wu, Y.-M. Activation of the Hippocampal LXR β Improves Sleep-Deprived Cognitive Impairment by Inhibiting Neuroinflammation. *Mol. Neurobiol.* **2021**, *58* (10), 5272–5288.

(68) Sun, T.; Li, Y.-J.; Tian, Q.-Q.; Wu, Q.; Feng, D.; Xue, Z.; Guo, Y.-Y.; Yang, L.; Zhang, K.; Zhao, M.-G.; Wu, Y.-M. Activation of liver X receptor β -enhancing neurogenesis ameliorates cognitive impairment induced by chronic cerebral hypoperfusion. *Exp. Neurol.* **2018**, *304*, 21–29.